RSC Advances

PAPER

View Article Online
View Journal | View Issue

Cite this: *RSC Adv.*, 2020, **10**, 25848

D–π–A azine based AIEgen with solvent dependent response towards a nerve agent†

Munusamy Sathiyaraj[a] and Viruthachalam Thiagarajan *[ab]

Received 4th June 2020
Accepted 2nd July 2020

DOI: 10.1039/d0ra04941g

rsc.li/rsc-advances

We developed a D–π–A based unsymmetrical azine molecule 4-((*E*)-((*E*)-(4-(dipropylamino)benzylidene) hydrazono)methyl)benzonitrile [**DPBN**] and studied its optical and aggregation induced emission properties. The **DPBN** molecule shows good aggregation induced emission (AIE) behaviour with 1157-fold fluorescence enhancement in the aggregated state. In addition to that, both colorimetric as well as fluorometric sensing studies revealed that **DPBN** selectively detects diethylchlorophosphate (**DCP**), a potent nerve agent. Interestingly, **DPBN** shows solvent dependent optical output in the presence of **DCP** *via* two different mechanisms. In the monomer state, it shows red shifted fluorescence enhancement along with color change from colorless to orange color *via* the formation of a new intramolecular charge transfer state in pure tetrahydrofuran (THF). In the aggregated state, **DPBN** shows blue shifted emission with fluorescence enhancement in THF–water mixture by protonation at the amine nitrogen centre. Thus, **DPBN** can be used as a diagnostic measure to selectively detect nerve agents like **DCP**. This study also paves the way for further development of molecular probes for nerve agents that would represent immense implications in various fields of chemistry and biology.

1. Introduction

Fluorescent materials play an important role in bioimaging and optoelectronics due to their rapid response, and high sensitivity and provide good time resolution, in-place operability and excellent repeatability.[1] Among the fluorescent materials, organic molecules have much attracted researchers due to the availability of room for various structural changes which in turn leads to materials with desired applications and properties.[2] Designing optical materials for biological applications is a challenging and demanding task. Chemists are interested to develop a fluorophore with longer wavelength emission for application in organic light emitting diodes (OLED) and biology.[3,4] The large planar π-conjugated organic fluorescent molecules can easily form the π–π stacking which may lead to non-radiative decay pathways, and this phenomenon is called aggregation caused quenching (ACQ). In the aqueous solution, ACQ based planar organic molecules are non-emissive or weakly emissive due to the formation of a greater number of stable aggregates. To overcome this drawback, Tang *et al.* reported a new aggregation induced emission (AIE) behaviour in 1-methyl-1,2,3,4,5-pentaphenylsilole molecule.[5] To date, several AIE molecules were reported such as tetraphenylethylene,[6,7] triphenylethylene,[8] salicylaldehyde azines,[9] siloles,[10] aza-benzanthrones[11] and cyanostilbenes,[12] and they have been utilized as building blocks to construct AIE active functional systems. Among them, azine based D–π–A molecules play an important role in fluorescent materials because of their convenient synthesis, tuning the emission wavelength depending on the substituents on azines, and high quantum efficiencies in the solid state.[9] Among them, only very few AIE based unsymmetrical azine molecules were reported due to their difficult way to get them mostly all the synthetic procedures lead to symmetrical azine derivatives.[9,13,14] AIE based fluorophores play a key role in the detection nerve agents.[15]

Organophosphorous compounds like sarin, tabun, soman are highly toxic nerve agents.[16] The reactive phosphate group of these molecules are able to interact with the hydroxyl groups of acetylcholinesterase irreversibly which further block the decomposition of acetylchloline creating a neurological imbalance, further it leads to the organ failure, paralysis of central nerve system and ultimate death.[15–17] Due to the extreme toxicity of these nerve agents, simulants like diethylcyanophosphate (DCNP), diisopropylfluorophosphate (DFP), diethylchlorophosphate (**DCP**) are used for the studies as they possess similar reactivity as real nerve agents and off less toxicity.[15] Gas chromatography-mass spectrometry, enzymatic assay, electrochemistry, ion mobility spectroscopy are some of the methods and they have been employed for their detection.[18–21] However, these methods suffer from disadvantages like low sensitivity and selectivity, non-portability and they are time consuming. The detection of these gaseous compounds by fluorescent

[a]*Photonics and Biophotonics Lab, School of Chemistry, Bharathidasan University, Tiruchirappalli-620 024, India. E-mail: v.thiagarajan@bdu.ac.in; vthiags@gmail.com; Tel: +91-4366-2407053*

[b]*Faculty Recharge Programme, University Grants Commission, New Delhi, India*

† Electronic supplementary information (ESI) available. See DOI: 10.1039/d0ra04941g

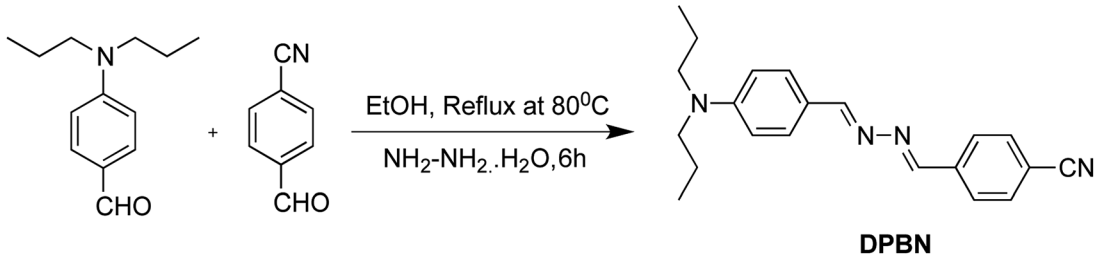

Scheme 1 Synthetic pathway of **DPBN**.

sensors is gaining importance due to their portability, cost-effective, and high selectivity and sensitivity.[15,22] Due to the high demand for the fluorescent probes to detect these nerve agents, several fluorescent probes including symmetrical azine derivatives were identified for their gas phase detection in the solid state.[15,23–27] Moreover most of the fluorophore used for sensing applications suffer from aggregation caused quenching phenomenon in the solid state which reduces the fluorescent intensity. In contrast, AIE paves the way for the solution and is a good candidate for solid state sensors.[28–30] In this context, we herein synthesize and present a new unsymmetrical azine molecule **DPBN** which shows an excellent selectivity to detect **DCP** in aqueous as well as non-aqueous media with different optical output *via* different sensing mechanisms.

2. Experimental section

2.1 Synthesis of 4-((*E*)-((*E*)-(4-(dipropylamino)benzylidene) hydrazono)methyl)benzonitrile [DPBN]

4-(Dipropylamino)benzaldehyde used for the synthesis of azine molecule was prepared by the earlier reported procedure.[31] To the one equivalent of 4-(dipropylamino)benzaldehyde in 5 mL of ethanol, one equivalent of hydrazine monohydrate dissolved in 5 mL of ethanol was added dropwise along with stirring. To the stirred mixture, one equivalent of 4-cyanobenzaldehyde dissolved in ethanol was added along with stirring. The final reaction mixture was refluxed for 6 h at 80 °C and then the formed product was filtered, washed several times with ethanol, and then dried (Scheme 1). The final dried product was recrystallized using dichloromethane–ethanol mixture and characterized using ^{1}H and ^{13}C NMR, and HRMS spectra (Fig. S1–S3†). ^{1}H NMR (400 MHz, $CDCl_3$) δ: 8.63 (s, 1H), 8.58 (s, 1H), 7.92 (d, 2H), 7.71 (d, 2H), 7.69 (d, 2H), 6.67 (d, 2H), 3.33 (t, 4H), 1.70 (m, 4H), 0.97 (t, 6H); ^{13}C NMR (400 MHz, $CDCl_3$) δ: 164.40, 157.57, 150.93, 139.01, 132.47, 130.96, 128.47, 120.19, 118.72, 113.42, 111.30, 52.82, 20.47, 11.47. HRMS (ESI-TOF) *m*/*z*: $[M + H]^+$ calcd for $C_{21}H_{25}N_4$, 333.2074; found: 333.2075

3. Results and discussion

3.1 Solvent effect

The absorption and emission studies of **DPBN** was carried out in different solvents with varying the polarity and presented in

Table 1 Photophysical data of **DPBN** in various solvents[a]

Solvent	λ_{abs} (nm)	λ_{emi} (nm)	Stoke's shift cm^{-1}	
			Shorter wavelength emission	Longer wavelength emission
Toluene	407	470, 500 (s)	3354	—
DCM	414	510	4547	—
THF	408	474, 500 (s)	3412	—
MeOH	411	563	—	6569
ACN	407	472 (s), 560	—	6713
DMF	413	473, 553	3072	6130

[a] s = shoulder peak.

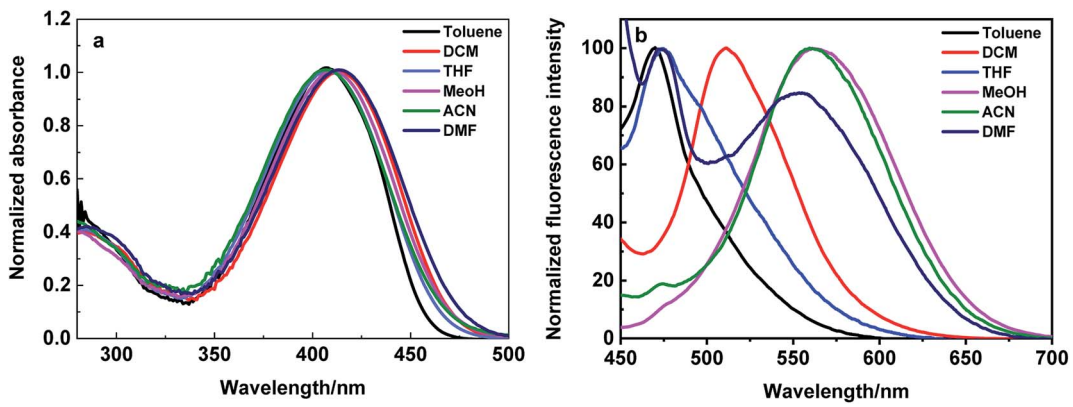

Fig. 1 (a) Absorption and (b) emission spectra of **DPBN** in different solvent.

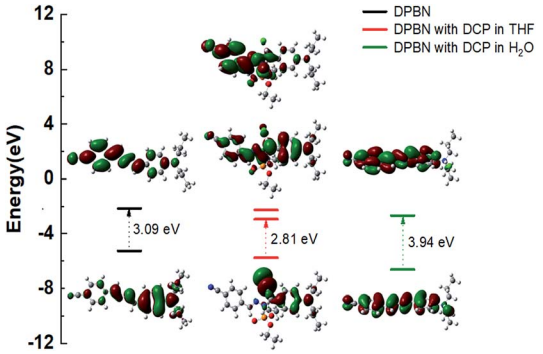

Fig. 2 Molecular orbital plots for the DPBN in the presence and absence of DCP.

Fig. 1, and the corresponding photophysical data were summarized in Table 1. The shorter wavelength absorption around 300 nm is assigned to the electronic transition within *N*,*N*-dipropylaniline moiety, while the longer wavelength absorption around 405 nm (Fig. 1a) is assigned to the charge transfer transition between the donor (*N*,*N*-dipropylamine) to the benzonitrile acceptor moiety. For better understanding of the ground state geometry and electronic structure, time dependent DFT calculation was carried out for **DPBN**. The highest occupied molecular orbital is localized on *N*,*N*-dipropylaniline moiety, whereas, lowest unoccupied molecular orbital is mainly distribute over benzonitrile and imine acceptor moieties. Fig. 2 shows the HOMO and LUMO orbitals of **DPBN** acquired using Gaussian B3LYP/6-31G* level.[32] In contrast to absorption spectrum, the emission spectrum recorded by exciting at the longer wavelength absorption maximum of **DPBN** shows dual fluorescence. The intensity and wavelength maximum of these two peaks depend upon the polarity of the solvent (Fig. 1b).

The **DPBN** shows shorter wavelength emission maximum around 470 nm and it is due to the charge transfer from the *N*,*N*-dipropylamine to the imine moiety[24,33] and the longer wavelength anomalous emission around 550 nm is due to the stabilized intramolecular charge transfer between the amine to benzonitrile moiety within the azine molecule. The shorter wavelength emission predominates in non-polar solvents, and the longer wavelength emission predominates in polar solvents. Stokes shift value calculated from different solvent and the value obtained in the range of 3000–6700 cm^{-1} depending upon the emission peak. This Stoke's shift values are increased with increasing solvent polarity and it clearly shows the different charge distribution in the excited state (S_1) as compared to ground state (S_0). The observed red shift's with increase in solvent polarity showed the intramolecular charge transfer takes place from donor to acceptor moieties.

3.2 Aggregation induced emission studies

The aggregation induced emission behaviour of **DPBN** was studied in different THF and water fractions (f_w), and the results are presented in Fig. 3. The absorption spectrum shows decrease in absorbance along with red shift in absorption

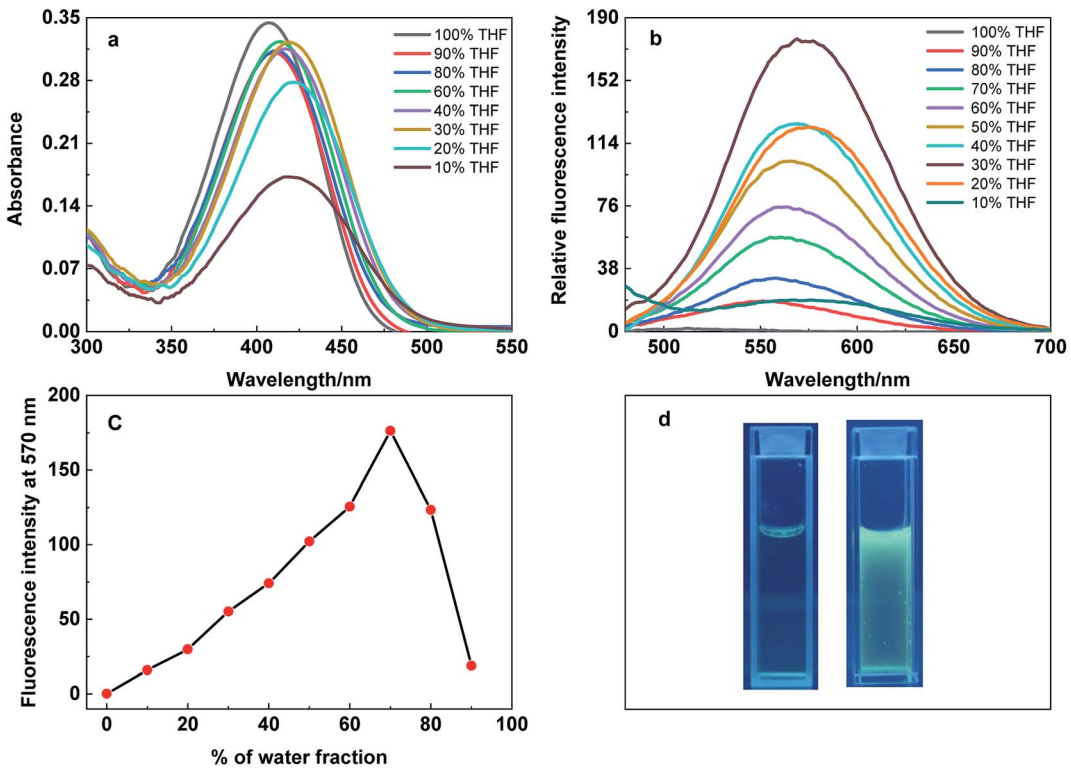

Fig. 3 (a) Absorption and (b) emission spectra of DPBN (10 μM) in different THF–water fraction, $\lambda_{exc} = 407$ nm; (c) plot of fluorescence intensity *vs.* water fraction; (d) DPBN in pure THF and 70% water fraction under 365 nm UV light illumination.

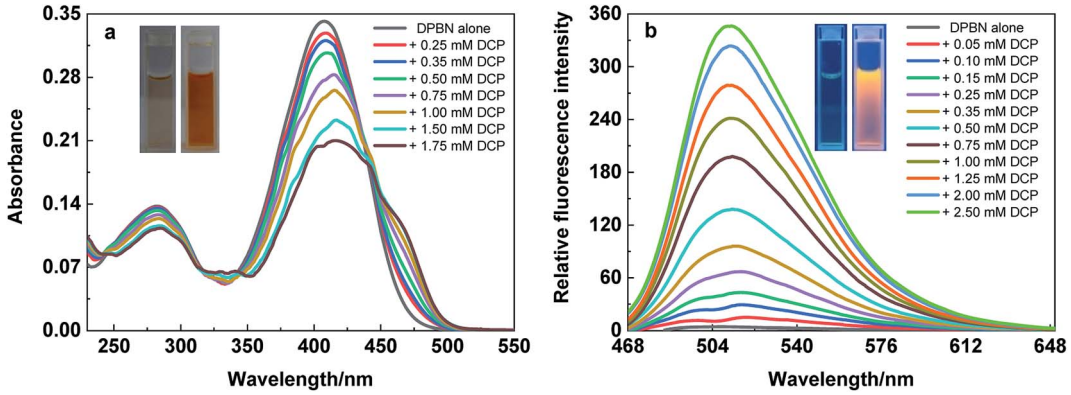

Fig. 4 (a) Absorption and (b) emission spectrum of **DPBN** (10 μM) in the presence and absence of **DCP** in pure THF. λ_{exc} = 440 nm.

maximum on increasing the water fraction. In contrast, the emission spectrum shows increase in emission intensity from the stabilized longer wavelength CT state with increase in water fraction until 70%. After 80% of water fraction, the aggregated molecules precipitate to form a greenish yellow coloured turbid solution which results in decrease in emission intensity. The decrease in absorbance after 80% of water fraction noticed in the absorption studies also validate the above mentioned fact. In the aggregated state, the longer wavelength CT state undergoes stabilization due to the restricted intramolecular rotation around C–N and N=N bonds that results in fluorescence enhancement.[33] The fluorescence enhancement was calculated from the ratio between the fluorescence intensity of **DPBN** in 30 : 70 THF–water mixture and in pure THF at 572 nm. The fluorescence enhancement for **DPBN** is found to be 1157 folds in the aggregated state in 70% of water fraction.

3.3 Detection of DCP in pure THF

The absorption studies of **DPBN** in the presence and absence of **DCP** has been revealed a significant change in the absorption spectrum in pure THF. As shown in Fig. 4a, the absorption maximum of **DPBN** at 407 nm decreases with the formation of a very broad absorption band, along with the formation of a new longer wavelength absorption around 460 nm with increase in **DCP** concentration. The formation of a clear isosbestic point at 440 nm with increase in **DCP** concentration proves that the interaction between **DCP** and **DPBN** in the ground state with a single equilibrium. The colour of the solution changed from colourless to orange colour within 60 seconds and was able to detect with our naked eye (Fig. 4a inset). As like the absorption spectrum, there is a formation of new emission peak at 513 nm in the presence of **DCP**, and the emission intensity of 513 nm peak increases with increase in **DCP** concentration (Fig. 4b). At higher **DCP** concentration, the longer wavelength emission is only visible (513 nm) due to higher intensity along with 203-fold fluorescence enhancement. The red shift in the absorption and emission maximum in the presence of **DCP** clearly indicates ICT based mechanism involved in the sensing process. Fig. 4b inset shows the 365 nm UV light illumination in the presence and absence of **DCP** in pure THF and it changes from very weak fluorescence to strong orange fluorescence with maximum emission at 513 nm. There is no such change in absorption and emission spectra were observed in the presence of other analytes such as tetrabutylammonium phosphate, triethyl phosphate, triethyl phosphite, thionyl chloride and acetyl chloride with **DPBN** in THF (Fig. S4†). It reflects, **DPBN** detects **DCP** in the highly selective and specific manner and the detection limit was determined from the fluorescence titration data based on a reported method[34] and found to be 200 nM in THF.

3.4 DCP detection mechanism in THF

The modulation of donor or acceptor abilities by an analyte in a charge transfer system leads to a significant change in the absorption as well as emission spectrum.[35–38] In the presence of

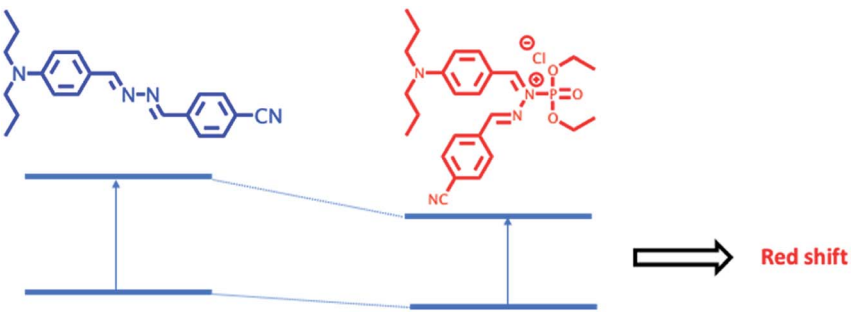

Scheme 2 Graphical representation of mechanism of **DCP** sensing by **DPBN** in pure THF.

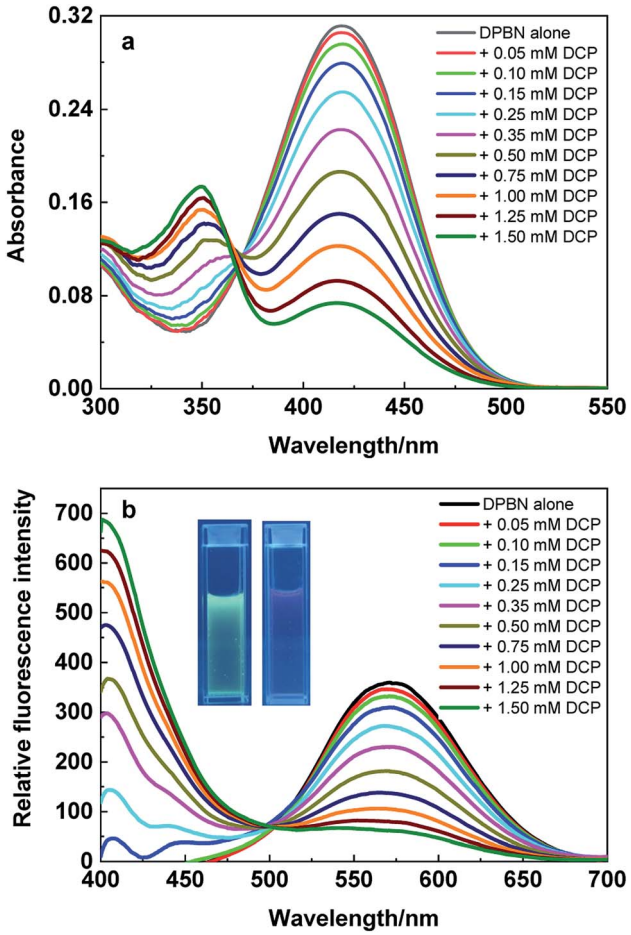

Fig. 5 (a) Absorption and (b) emission spectrum of DPBN (10 μM) with varying DCP concentration (0 to 1.50 mM) in THF/water (3 : 7) mixture, λ_{exc} = 368 nm.

DCP, phosphorylation takes place at the imine nitrogen close to the donor moiety of **DPBN** that results in orange colour product and it shows a new absorption around 460 nm. In **DPBN**, imine nitrogen acts as a good electron rich centre as well as good nucleophile and it easily undergoes phosphorylation by a **DCP** electrophile. After phosphorylation, this moiety acts as a strong withdrawing group which in turn changes the ICT pathway.[15,39]

The interaction between the **DCP** and **DPBN** is presented in Scheme 2.

If the **DCP** interacts with *N*,*N*-dipropylamine moiety instead of imine nitrogen will lead to decrease in electron donating ability of donor moiety that in turn leads to blue shift in the absorption and emission spectrum in the presence of **DCP**. The observation of red shift in the absorption as well as emission spectrum in the presence of **DCP** confirms that the **DCP** interacts only with the imine nitrogen of **DPBN**. In order to confirm the mode of interaction between **DPBN** and **DCP**, ^{1}H NMR titration carried out in $CDCl_3$-d_6 and presented in Fig. S5.† In the absence of **DCP**, **DPBN** shows two imine protons signal at 8.62 (s, 1H) and 8.57 (s, 1H) ppm and aromatic protons near to the donor moiety at 7.91 (d, 2H), 7.71 (d, 2H), 7.69 (d, 2H), 6.67 (d, 2H) ppm. On increasing the **DCP** concentration form 0.5 to 1 equivalent, both the imine protons and aromatic protons closer to *N*,*N*-dipropyl moiety undergo downfield which confirms the above said mechanism. In order to verify the role of *N*,*N*-propylamine, similar kind of absorption studies were carried out with a control azine molecule BA, without the donor and acceptor moieties (Fig. S6 and S7†). There is no significant change that was observed in the presence of **DCP** in THF. It clearly proves that *N*,*N*-dipropyl donor moiety plays a key role in the phosphorylation mechanism.

3.5 Detection of DCP in aqueous media

In order to study the sensing behaviour of aggregated **DPBN** in aqueous media same set of experiments were carried out in THF/water (3 : 7) mixture and presented in Fig. 5. In the absence of **DCP**, **DPBN** shows the absorption and emission peak at 417 nm and 570 nm respectively due to the presence of aggregated molecules in THF/water (3 : 7) mixture. On increasing the concentration of **DCP** leads to the formation of a new absorption band at 350 nm and the absorbance of 417 nm band decreases along with a clear isosbestic point at 368 nm. The blue shift in the absorption maximum clearly confirms the destabilization of ICT transition of **DPBN** molecule in the presence of **DCP**. As similar to the absorption spectra, the emission spectra presented in Fig. 5b also shows the formation of new emission peak at 406 nm along with the decrease in emission intensity of 570 nm peak in the presence of **DCP** in THF/water (3 : 7) mixture. The formation of isoemissive point at 498 nm and 164 nm blue shift in the

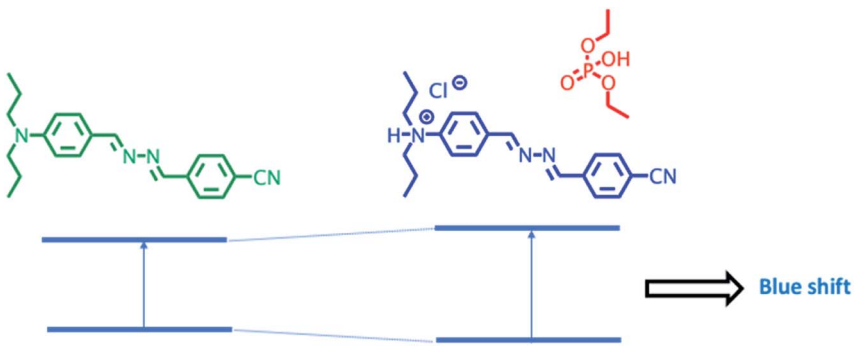

Scheme 3 Graphical representation of mechanism of DCP sensing by DPBN in aqueous media.

emission spectrum in the presence of **DCP** confirms the presence of single equilibrium and strong destabilization of ICT transition in the excited state. Fig. 5b inset shows a change in fluorescence from green to violent with **DCP** in THF/water (3 : 7) mixture at 365 nm UV illumination. There is no significant change in absorption and emission spectra were observed in the presence of tetrabutylammonium phosphate, triethyl phosphate, triethyl phosphite, thionyl chloride and acetyl chloride with **DPBN** in THF/water (3 : 7) mixture (Fig. S8†). The detection limit of **DCP** from the fluorescence titration in THF/water (3 : 7) mixture is found to be 106 μM.

3.6 DCP detection mechanism in aqueous media

DCP undergoes hydroxylation in aqueous media to form a diethyl phosphate and hydrochloric acid. The formed hydrochloric acid protonate the nitrogen of *N*,*N*-dipropylamine donor moiety which in turn destabilize the ICT transition between *N*,*N*-dipropylamine donor moiety to the benzonitrile acceptor moiety of **DPBN** molecule. Scheme 3 represents the suppression of donating ability of *N*,*N*-dipropylamine moiety after protonation at amine nitrogen.

In order to confirm the above said mechanism, pH studies were carried out in the pH range of 9 to 1 for **DPBN** molecule in 30 : 70 THF–water mixture and the spectra were presented in Fig. 6. The solution pH was adjusted by adding HCl or NaOH to THF/water (3 : 7) mixture and measure the pH using pH meter. To the adjusted pH solution, **DPBN** was added and recorded the absorption and emission spectrum. Until the pH 3.5, there is no significant change in the absorption as well as emission spectrum of **DPBN** molecule. On further decrease in pH leads to the formation of a new absorption peak at 356 nm and decrease in absorbance of 419 nm peak along with a isosbestic point at 373 nm. The corresponding emission spectrum recorded by exciting at the isosbestic point shows decrease in emission intensity of 570 nm along with the formation of new emission peak at 406 nm as similar to the one observed in the presence of **DCP**. This result confirms that the protonation of **DPBN** is responsible for the formation of new blue shifted absorption as well as emission observed in the presence of **DCP** in THF/water (3 : 7) mixture. The lower fluorescence enhancement observed for **DPBN** in acidic pH at 406 nm compared to the presence of **DCP** may be due to the more pronounced inner filter effect (self-adsorption of protonated species) in acidic media. The earlier pH studies on the control azine molecule BA confirms that the protonation occurs only at the amine nitrogen and not at the imine nitrogen.[33] In order to test the real time application of **DPBN** probe, a test-strip based detection assay was developed to detect **DCP** vapor using Whatman filter paper. Whatman test strips were dipped into the THF solution of **DPBN** and air-dried. The color the test strip changes from yellow to orange immediately after exposure to the **DCP** vapor (Fig. S9†). It proves that the **DPBN** based test strips could be used to detect **DCP** vapor qualitatively for rapid detection.

TD-DFT calculations were carried out in THF and water using PCM solvation method to understand the relationship between the absorption spectra and the associated electronic transition in the presence of **DCP** (Fig. 2).[32] The results confirm the proposed sensing mechanisms in both THF and THF–water mixture. In THF, major contributions from both HOMO to LUMO as well as HOMO to LUMO+1 was observed and it explains the experimentally observed broad absorption spectrum in the presence of **DCP** in THF. Furthermore, the HOMO is localized on *N*,*N*-dipropylamine moiety and the LUMO is localized both on benzonitrile as well as phosphate moiety. In water, the theoretical band gap energy confirm that the formation of new blue shifted absorption in the presence of **DCP** is originated from the protonated **DPBN** and has excitation energy of 3.94 eV which is comparable to that of the experimental energy of 3.54 eV in THF–water mixture. All theoretical results correlated well with the experimentally observed results.

3.7 Binding mode and sensing mechanism of DPBN in different solvent environment

DCP sensing studies were carried out with **DPBN** molecule both in aggregated and monomer forms. In THF–water mixture **DPBN** molecules are in the aggregated form whereas in pure THF, **DPBN** molecules are in the monomer form. In pure THF, phosphorylation takes place at the imine nitrogen close to the donor moiety of **DPBN** that results in stabilization of intramolecular charge transfer which in turn leads to red shift (Fig. 7a). In THF/water (3 : 7) mixture, due to the hydroxylation of **DCP** the formed hydrochloric acid protonate the nitrogen of

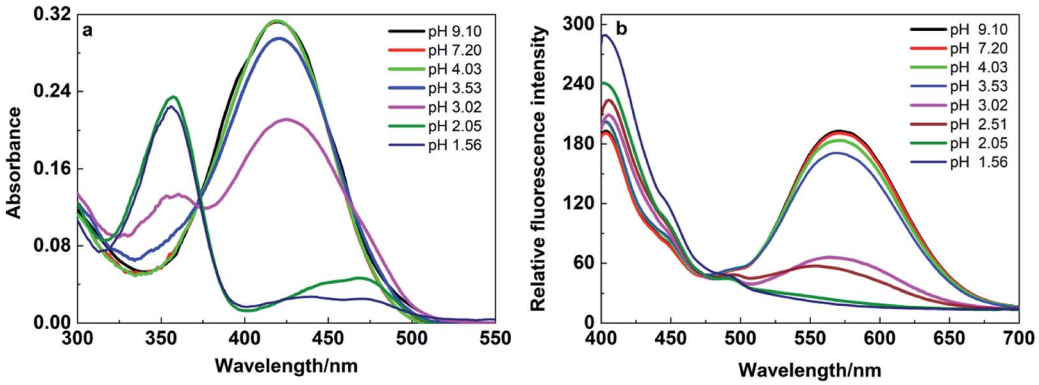

Fig. 6 (a) Absorption and (b) emission spectrum of **DPBN** (10 μM) in THF/water (3 : 7) mixture at different pH, λ_{exc} = 368 nm.

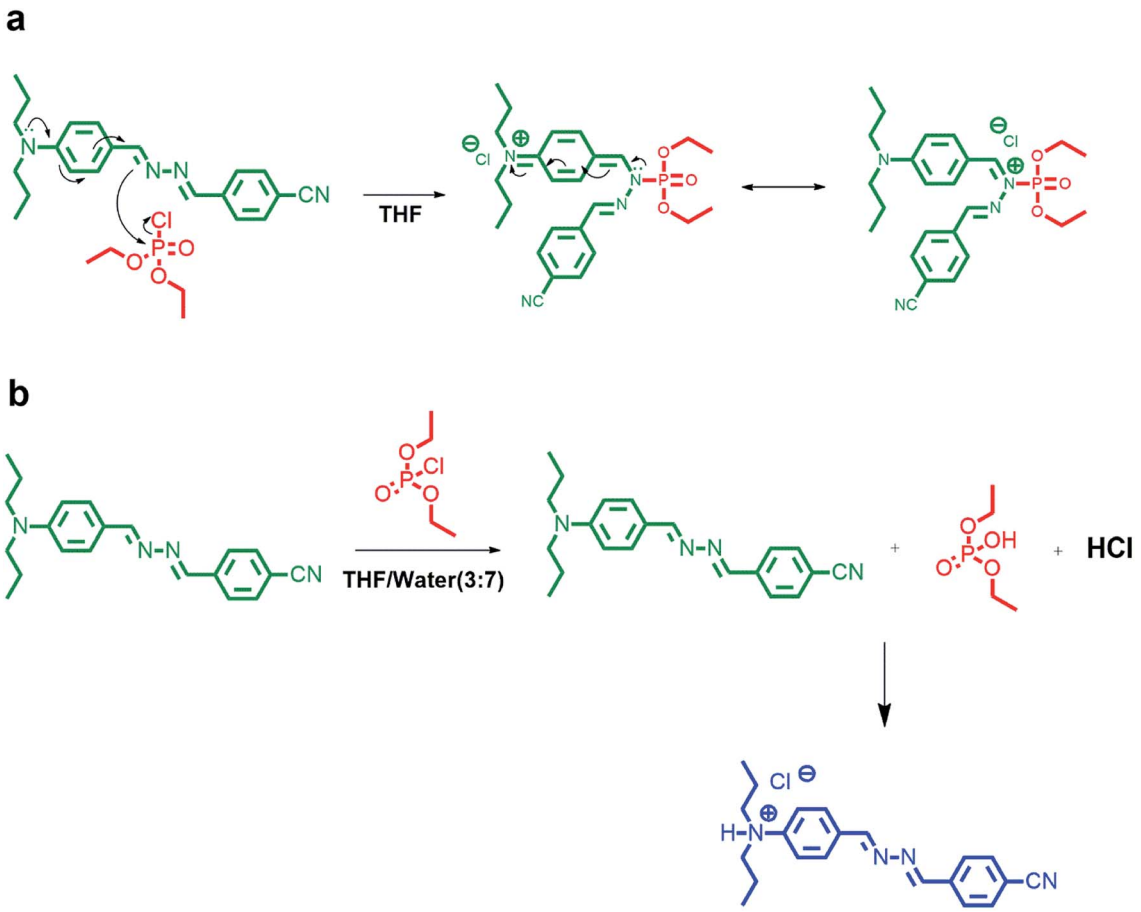

Fig. 7 Plausible sensing mechanism of **DPBN** with **DCP** in different solvent environment (a) THF (b) THF/water (3 : 7) mixture.

N,*N*-dipropylamine donor moiety which in turn decrease the donating capability of the donor that results in the destabilization of ICT transition leads to blue shift (Fig. 7b).

4. Conclusion

In this work, we have reported the photophysical and AIE properties of D–π–A based **DPBN** azine molecule. In the aggregated state, **DPBN** shows 1157 fold fluorescence enhancement in THF–water mixture. The **DPBN** detects **DCP** with high sensitivity and selectivity in both monomer as well as in aggregated forms. In pure THF, phosphorylation occurs at the imine nitrogen that leads to new red shifted absorption and emission spectra by the formation of new ICT state. In THF–water mixture, **DCP** undergoes hydroxylation to form a diethyl phosphate and hydrochloric acid. The formed hydrochloric acid protonate the amine nitrogen results in the formation of new blue shifted absorption and emission spectra by destabilization of ICT state. In both solvent environment, **DPBN** shows fluorescence enhancement due to the change in the ICT state *via* two different mechanisms.

Conflicts of interest

There are no conflicts of interest to declare.

Acknowledgements

This research was supported by Science and Engineering Research Board (SERB), New Delhi, India [grant no. YSS/2014/00026] and DST Nanomission [grant no. DST/NM/NB/2018/10(G)]. VT thanks UGC, New Delhi, for a start-up grant and UGC FRP Faculty Award [F. 4-5(24-FRP)/2013(BSR)]. MS acknowledges UGC-RFSMS for fellowship. We thank DST, New Delhi for providing 400 MHz NMR, TCSPC and HRMS facilities under FIST program. We thank Dr K. Thirumoorthy, VIT for the theoretical calculations.

References

1 F. Ren, J. Shi, B. Tong, Z. Cai and Y. Dong, *Mater. Chem. Front.*, 2019, **3**, 2072–2076.
2 H. J. Chen, C. Y. Chew, E. H. Chang, Y. W. Tu, L. Y. Wei, B. H. Wu, C. H. Chen, Y. T. Yang, S. C. Huang, J. K. Chen, I. C. Chen and K. T. Tan, *J. Am. Chem. Soc.*, 2018, **140**, 5224–5234.
3 S. Kundu, B. Sk, P. Pallavi, A. Giri and A. Patra, *Chem.–Eur. J.*, 2020, **26**, 5557–5582.
4 M. Gao, F. Yu, C. Lv, J. Choo and L. Chen, *Chem. Soc. Rev.*, 2017, **46**, 2237–2271.

5 B. Z. Tang, X. Zhan, G. Yu, P. P. Sze Lee, Y. Liu and D. Zhu, *J. Mater. Chem.*, 2001, **11**, 2974–2978.
6 J. Shi, Q. Deng, Y. Li, M. Zheng, Z. Chai, C. Wan, Z. Zheng, L. Li, F. Huang and B. Tang, *Anal. Chem.*, 2018, **90**, 13775–13782.
7 H. Wang, X. Ji, Y. Li, Z. Li, G. Tang and F. Huang, *J. Mater. Chem. B*, 2018, **6**, 2728–2733.
8 H. Shi, D. Xin, X. Gu, P. Zhang, H. Peng, S. Chen, G. Lin, Z. Zhao and B. Z. Tang, *J. Mater. Chem. C*, 2016, **4**, 1228–1237.
9 S. Kagatikar and D. Sunil, *J. Mol. Liq.*, 2019, **292**, 111371–111398.
10 Z. Zhao, B. He and B. Z. Tang, *Chem. Sci.*, 2015, **6**, 5347–5365.
11 Q. Zang, J. Yu, W. Yu, J. Qian, R. Hu and B. Z. Tang, *Chem. Sci.*, 2018, **9**, 5165–5171.
12 S.-Y. Chen, Y.-W. Chiu and G.-S. Liou, *Nanoscale*, 2019, **11**, 8597–8603.
13 J. Tong, K. Zhang, J. Wang, H. Li, F. Zhou, Z. Wang, X. Zhang and B. Z. Tang, *J. Mater. Chem. C*, 2020, **8**, 996–1001.
14 M. Mathivanan, B. Tharmalingam, C. H. Lin, B. V. Pandiyan, V. Thiagarajan and B. Murugesapandian, *CrystEngComm*, 2020, **22**, 213–228.
15 L. Chen, D. Wu and J. Yoon, *ACS Sens.*, 2018, **3**, 27–43.
16 N. Munno, *Environ. Health Perspect.*, 1994, **102**, 18–37.
17 S. Costanzi, J. H. Machado and M. Mitchell, *ACS Chem. Neurosci.*, 2018, **9**, 873–885.
18 R. M. Black, R. J. Clarke, R. W. Read and M. T. J. Reid, *J. Chromatogr. A*, 1994, **662**, 301–321.
19 F. N. Diauudin, J. I. A. Rashid, V. F. Knight, W. M. Z. W. Yunus, K. K. Ong, N. A. M. Kasim, N. A. Halim and S. A. M. Noor, *Sensing and Bio-Sensing Research*, 2019, **26**, 100305.
20 V. V. Singh, *Electroanalysis*, 2016, **28**, 920–935.
21 M. A. Makinen, O. A. Anttalainen and M. E. T. Sillanpaa, *Anal. Chem.*, 2010, **82**, 9594–9600.
22 X. Zhou, Y. Zeng, L. Chen, X. Wu and J. Yoon, *Angew. Chem., Int. Ed.*, 2016, **55**, 4729–4733.
23 S. Sarkar and R. Shunmugam, *Chem. Commun.*, 2014, **50**, 8511–8513.
24 Y. Fu, J. Yu, K. Wang, H. Liu, Y. Yu, A. Liu, X. Peng, Q. He, H. Cao and J. Cheng, *ACS Sens.*, 2018, **3**, 1445–1450.
25 N. Kwon, Y. Hu and J. Yoon, *ACS Omega*, 2018, **3**, 13731–13751.
26 X. Zhou, S. Lee, Z. Xu and J. Yoon, *Chem. Rev.*, 2015, **115**, 7944–8000.
27 S. K. Sheet, B. Sen and S. Khatua, *Inorg. Chem.*, 2019, **58**, 3635–3645.
28 Z. Song, W. Zhang, M. Jiang, H. H. Sung, R. T. Kwok, H. Nie, I. D. Williams, B. Liu and B. Z. Tang, *Adv. Funct. Mater.*, 2016, **26**, 824–832.
29 A. Shao, Y. Xie, S. Zhu, Z. Guo, S. Zhu, J. Guo, P. Shi, T. D. James, H. Tian and W. H. Zhu, *Angew. Chem., Int. Ed.*, 2015, **54**, 7275–7280.
30 H. Wang, D. Chen, Y. Zhang, P. Liu, J. Shi, X. Feng, B. Tong and Y. Dong, *J. Mater. Chem. C*, 2015, **3**, 7621–7626.
31 Y. Wang, T. Liu, L. Bu, J. Li, C. Yang, X. Li, Y. Tao and W. Yang, *J. Phys. Chem. C*, 2012, **116**, 15576–15583.
32 M. J. Frisch, G. W. Trucks, H. B. Schlegel, G. E. Scuseria, M. A. Robb, J. R. Cheeseman, G. Scalmani, V. Barone, B. Mennucci, G. A. Petersson, H. Nakatsuji, M. Caricato, X. Li, H. P. Hratchian, A. F. Izmaylov, J. Bloino, G. Zheng, J. L. Sonnenberg, M. Hada, M. Ehara, K. Toyota, R. Fukuda, J. Hasegawa, M. Ishida, T. Nakajima, Y. Honda, O. Kitao, H. Nakai, T. Vreven, J. A. Montgomery, J. E. Peralta, F. Ogliaro, M. Bearpark, J. J. Heyd, E. Brothers, K. N. Kudin, V. N. Staroverov, R. Kobayashi, J. Normand, K. Raghavachari, A. Rendell, J. C. Burant, S. S. Iyengar, J. Tomasi, M. Cossi, N. Rega, J. M. Millam, M. Klene, J. E. Knox, J. B. Cross, V. Bakken, C. Adamo, J. Jaramillo, R. Gomperts, R. E. Stratmann, O. Yazyev, A. J. Austin, R. Cammi, C. Pomelli, J. W. Ochterski, R. L. Martin, K. Morokuma, V. G. Zakrzewski, G. A. Voth, P. Salvador, J. J. Dannenberg, S. Dapprich, A. D. Daniels, O. Farkas, J. B. Foresman, J. V. Ortiz, J. Cioslowski, and D. J. Fox, Gaussian, Inc., Wallingford CT, 2009.
33 M. Sathiyaraj, K. Pavithra and V. Thiagarajan, *New J. Chem.*, 2020, **44**, 8402–8411.
34 D. Tamilarasan, R. Suhasini, V. Thiagarajan and R. Balamurugan, *Eur. J. Org. Chem.*, 2020, 993–1000.
35 V. Thiagarajan, C. Selvaraju, E. J. Padma Malar and P. Ramamurthy, *ChemPhysChem*, 2004, **5**, 1200–1209.
36 V. Thiagarajan, P. Ramamurthy, D. Thirumalai and V. T. Ramakrishnan, *Org. Lett.*, 2005, **7**, 657–660.
37 S. Paul, P. Ghosh and P. Roy, *New J. Chem.*, 2020, **44**, 5784–5791.
38 Y.-C. Cai and Q.-H. Song, *ACS Sens.*, 2017, **2**, 834–841.
39 S. Royo, A. M. Costero, M. Parra, S. Gil, R. Martinez-Manez and F. Sancenon, *Chem.–Eur. J.*, 2011, **17**, 6931–6934.